Digital image processing techniques applied to pressure analysis and morphological features extraction in footprints.

F J Buchelly[1, 2, 3], D Mayorca[3], V Ballarín[1] and J Pastore[1]

[1] Laboratorio de Procesamiento Digital de imágenes, ICyTE (Instituto de Investigaciones Científicas y Tecnológicas en Electrónica) Facultad de Ingeniería, Universidad Nacional de Mar del Plata, Argentina
[2] Consejo Nacional de Investigaciones Científicas y Técnicas - CONICET
[3] Grupo de Óptica y Láser, Departamento de Física, Universidad del Cauca, Colombia

E-mail: fbuchelly@gmail.com

Abstract. This paper shows the correlation between foot morphology and pressure distribution on footplant by means of a morphological parameters analysis and pressure calculation. Footprint images were acquired using an optical pedobarograph and then processed for obtaining binary masks and intensity images in gray scale. Morphological descriptors were obtained from the binary images and the Hernandez Corvo (HC) index was automatically calculated for determine the type of foot. Pressure distributions were obtained from gray scale images making a correspondence between light intensity in footprints and pressure. Pressure analysis was performed by finding the maximum pressure, the mean pressure and the ratio between them that determines the uniformity of the distribution. Finally, a high correlation was found between this ratio and the type of foot determined by HC index.

1. Introduction

Obtaining footprint features is important issue in health and sports, because it permits to study pathologies related to foot morphology [1] [2], human locomotion [2] [4], or even in detecting risks produced by diabetes [5]. These pathology diagnostics are decisive in many disciplines like preventive medicine [6], clinical medicine [7], orthopedics [8], sports medicine [9] [10], and other.

Morphological and pressure features are data of medical interest. Currently, morphology features are visually obtained on footprint images in manual way [10], and also in semiautomatic way [11]. There are different forms of obtaining a person's footprint. Lara et al. [9] show some of them. Commonly, ink based methods are used, in which skin is put in contact with a paper sheet or some film. The patients not only feel uncomfortable with this procedure, but it is possible to make mistakes obtaining footprint images because diagnoses are subjective and it´s difficult to estimate pressure values.

A different system is a parallelepiped footprint viewer, or podoscope, with a flat glass surface in which a person keeps a vertical position supporting both feet, like is used in Oller [3]. In that work, fluorescent lamps emit yellow light at both sides of the glass, showing a luminous footprint when the total internal reflection condition (TIR condition) is eliminated by contact of the skin and glass. A similar version, proposed by Buchelly et al. [2] and Mayorca [5] uses green light, instead of yellow, that improves footprint intensity, due to radiation absorption of the glass that minimizes its value for near green wavelengths, allowing simpler Digital Image Processing.

Pressure distribution measurement can be made by sensor arrays [12] [13]. Usually, their spatial resolution is poor and can lose information about foot form in places where pressure value is low. Some other works [2] study feet morphology and pressure using different devices. Bates et al. [14] shows that geometry of a footprint, done in a compliant material, is related to pressure distribution. According to the previous conclusion, using a podoscope like the ones described in [2] and [5] also allows to determine the pressure of each point in a foot plant considering that skin roughness is deformed depending on the supported pressure. This deformation influences strongly the light intensity and allows integrate both devices in one called "pedobarograph".

Following the previous ideas, in this work we propose a comparative analysis of Digital Image Processing techniques used to automatically determining morphological parameters associated to each type of foot and pressure distribution in footprint images acquired from a pedobarograph device, respect to similar previous works.

2. Foot pathologies

From footprint data it is possible to make the following pathological studies.

2.1. Footprint morphology

There are several classifications of feet morphologies. One of them is the rank from plane foot to extreme cavus foot. Figure 1 shows examples of this rank. Each one produces a particular footprint and pressure distribution, affecting the gait and making feel more or less pain when the person stands in two feet. An intermediate interval between these extreme states is considered as normal foot.

Figure 1. Example of footprints of plane foot (up) in different grades, normal foot (medium left) and cavus foot (down). Image taken from [15]

2.1.1. Plane foot

A plane foot occurs when the decreasing of the plant arc is below normal values according to the Costa-Bartani angle and the location of scaphoid bone respect to the Feiss line. The ball is configured depending on these parameters, modifying the support points and the plant morphology [16].

2.1.2. Cavus foot

The cavus foot is often characterized by a ball accentuation due to the height of the longitudinal arcs. The distribution of pressure on the floor results perturbed by the oncoming of the anterior and posterior supports as well as the reduction of the support surface, mainly at the expense of the lateral border, which serves of basis for podoscopic classification of cavus feet [17].

2.1.3. Determining type of foot

Some authors [5] [9] [10] [11] [18] use some indexes that permit assign a value to each type of foot by its respective footprint. Some of them are: Clarke's angle, Chippaux`s angle, Arc Index, and others. However, the most used is the Hernandez Corvo (HC) index, also mentioned in the previous references. In order to assess the HC index, the following steps are performed [9]

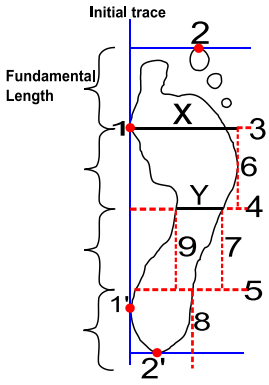

Figure 2. Hernandez Corvo procedure for footprint assessment.

- Mark two points in the inner salience (1 and 1') and do the "initial trace", joining both points
- Mark a point in the most anterior part of the footprint (including toes) and other in the most posterior point (2 and 2')
- Trace perpendicular lines to 2 and 2' respect to the initial trace. The distance between this trace and point 1 is the "fundamental length" and it has to be taken many times as possible on the initial trace (3, 4 and 5)
- Trace a line perpendicular to 3, crossing by the outer point of the footprint, and other two lines in similar way perpendicular to 4 and 5 in the outer part (6, 7 and 8, respectively). The distance between initial trace and 6 is X (metatarsial width); the distance between 9 and 7 is Y (extern arc, support surface in the middle of foot)
- Type of foot is obtained using Equation 1:

$$HCI = 100 * \frac{(X-Y)}{X} \quad (1)$$

HC index value classify foot in following percent ranges [10]

Table 1. Type of foot depending on HCI value.

IHC (%)	TYPE OF FOOT
0-34	Plane
35-39	Plane-Normal
40-54	Normal
55-59	Cavus-Normal
60-74	Cavus
75-84	High Cavus
85-100	Extreme Cavus

2.2. Pressure Distribution

The barometric parameters of foot are not independent of the morphology. The simplest example is the variation of pressure in different types of footprints determined by HC index. In extreme cavus foot, standing people feel more pain because corporal weight is supported by a smaller area. Another case in which morphology is related to pressure is Hallux Abductus Valgus (HAV) or "bunion", where not only the deformation of foot causes nuisance but also changes pressure distribution [19].

On the other hand, plant pressure analysis allows determining not only the morphologic pathologies, but also diabetic foot associated with diabetes mellitus. Among risk factors that can become in diabetic foot, the main pathology is the occurrence of abnormal pressure regions in foot [20] and redistribution

of maximum pressure points. Those signs and many others may allow the generation of ulcers and even amputation [21] [22].

3. Methodology

The proposed processing system is summarized in figure 3

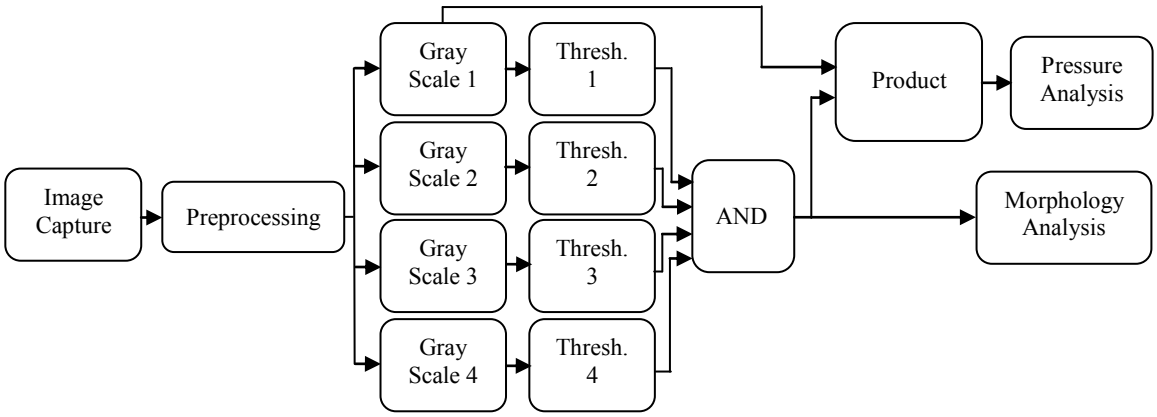

Figure 3. Flowchart that describes the general steps of the proposed methodology.

3.1. Image acquisition

In this work, a pedobarograph was fabricated to generate visible footprints, similar as the proposed in works [2] [5] [11] [23] [24] [25]. Its image formation system is described in figure 4.

Some of the mentioned devices use a film between foot skin and glass (or acrylic) with the purpose to avoid the light noise of the environment and reduce the dependency between the generated luminosity and the skin humidity. In spite of these advantages, using that material implies other kinds of noise and disadvantages because of its texture (loss of information), adherence with acrylic or glass, problems due to its thickness, and other [23]. For that reasons, this work doesn't use a transducer film, it makes footprint detection by applying different transformations to grayscale and creating binary masks by means of thresholding.

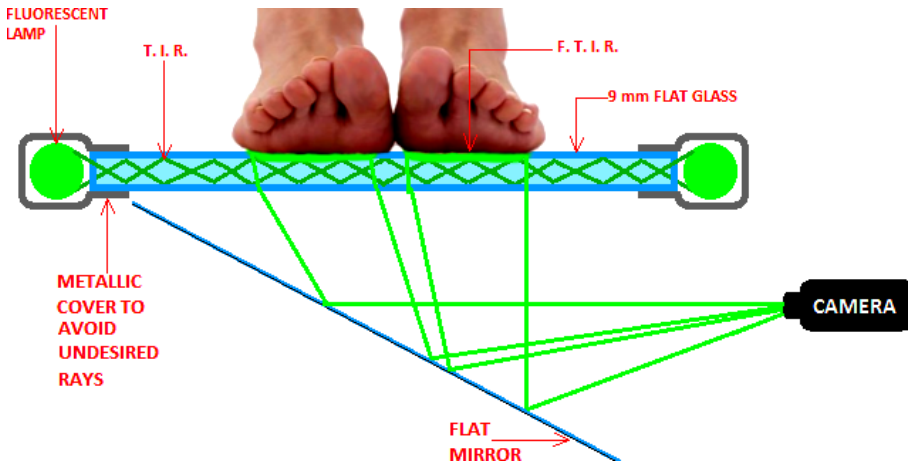

Figure 4. Image acquisition system by means of frustrating total internal reflection of light.

3.2. Preprocessing

The main objective in many Digital Image Processing applications is to measure parameters from the real world. In this case, it is necessary that the geometry of the acquired footprint image corresponds

to the geometry of flat image in glass for determining morphological features (lengths, areas) correctly. The camera was calibrated to correct optical distortions (radial, tangential, center deviation) produced by the camera lens [26] [27]. The camera parameters were obtained and correction model was generated by using a chessboard pattern. Additionally, it was needed to perform a geometric transform because of the camera position and using a flat mirror introduces perspective effects.

Sometimes noise filtering is used to avoid false detection and abrupt changes in gray levels. However, low pass filters mix light from FTIR with ambient light, affecting the footprint detection. Low pass filters are used later, after footprint is detected, to facilitate the study of pressure distribution. All the algorithms described below were developed in MatLab®.

3.3. Transformation to grayscale

This step is based on the use of RGB and HSV color spaces, having accounted the meaning of green color over all other. Mayorca [5] use an opaque transducer film to simplify the detection with a gray background and a green footprint, allowing only to intensity value and saturation value define the threshold method (V and S in HSV space). In this work, that method was omitted because of the non uniformity of background. Four independent transforms were used to highlight the footprint regions, instead. These transforms are explained in following sections, considering a color pixel as a three dimensional vector whose values in each component are two dimension functions (color planes) of spatial coordinates (Equations 2 and 3) and a gray scale pixel is the value of a two dimension function of spatial coordinates, resulting of any operation with color planes. The range of gray levels are normalized (from 0 to 1) instead of the usual (0 to 255) range.

$$I_{RGB}(x,y)=(R(x,y), G(x,y), B(x,y)) \quad (2)$$
$$I_{HSV}(x,y)=(H(x,y), S(x,y), V(x,y)) \quad (3)$$

3.3.1. Subtraction of red and blue values

The first method of green highlighting is the one used in references [2] [11], defined by equation 4.

$$\mathrm{Gray}_1(x,y) = G(x,y) - 0.5R(x,y) - 0.5B(x,y) \quad (4)$$

3.3.2. Gaussian of Hue values

Hue plane of HSV space is transformed to an intensity distribution according to Gaussian function with a mean in green ($\overline{H}$=1/3), defined by equation 5, and with an adjust factor f(x,y).

$$\mathrm{Gray}_2(x,y) = \exp\left(-\frac{(H(x,y)-0.\overline{3})^2}{\sigma^2}\right).f(x,y) \quad (5)$$

3.3.3. Subtraction of mean RGB from V value

In HSV space, V is defined as the maximum of R, G, and B [28], then there is a high difference between V and the mean of R, G, and B when one of them is 1 and the other values are 0. In the other hand, the difference is low if R, G and B are similar. This difference is defined by equation 6.

$$\mathrm{Gray}_3(x,y) = V(x,y) - \mathrm{mean}(R,G,B) \quad (6)$$

3.3.4. Comparison between R, G, B

As it was shown previously, the predominant color in footprint is green, although it can be mixed with a few of blue or red. Without compare proportions of blue and red present in a footprint, a fourth grayscale image can be defined under the condition given by equation 7.

$$\mathrm{Gray}_4(x,y) = \begin{cases} G, \text{if } G > \alpha R \text{ ^ } G > \beta B \\ 0, \quad \text{otherwise} \end{cases} \quad (7)$$

In equation 7, α and β are adjust constants, fixed for all images. For this work these values are α =1.5 and β =1 and were found experimentally.

3.4. Thresholding and Morphological operations

After gray scale transformations are performed, each image is thresholded with an optimum value obtained empirically. Although every gray scale image show an intensity pattern, where the brightest pixels represent green regions in the original image, the results are not the same. The obtained binary masks usually are different and a definitive mask by means of a logical AND operation was generated. Thus, both noise and morphological differences are eliminated.

Occasionally, some isolated small regions still remain, or some borders have defects or connected objects have holes. These aspects were corrected using morphological operations. We applied an opening followed by closing to smooth borders [29], delete isolated and small undesired particles. We used a disk structuring element. Finally, an algorithm of holes filling is applied.

3.5. Foot morphology analysis

In this work, the equivalence between physical lengths on the glass surface and discrete lengths in the images was calculated (1 pixel-length=0.054cm). This conversion parameter is the same for vertical and horizontal directions in images. With this value, is possible to measure patient's feet length and width, as well as orientation of the feet, arc length, support area, although the decisive parameter to determine the type of foot was Hernandez Corvo Index, automatically calculated.

First step in determining HC index was to align the images of each foot independently along of the major axes of the feet, in approximation of the principal length direction. This line was in vertical orientation in each image. Then, X and Y were found like horizontal lines and HCI was determined using Equation 1. Nevertheless, that procedure sometimes causes errors due to the unsupervised detection of extern in the foot arc. Because of this, two alternative methods were performed for the HCI determination:

- Second method: taking the X value as the foot width and the Y value as the width of the footprint at the medium height between points 2 and 2'.
- Third method: taking the X value as the maximum horizontal width in the anterior part of foot, taking the X' value as the maximum horizontal width in the posterior part of foot and the Y value as the minimum horizontal width between X and X'.

The developed system displays HCI calculation using the three methods and the average value.

3.6. Pressure analysis

A useful intensity distribution $I_{green}(x,y)$ is obtained by multiplying the generated binary mask and a gray scale image. The best way to represent the variation of the green intensity in footprints was $Gray_1$ (See equation 4). The image $Gray_2$ may have high values even if the green intensity is low, because it is calculated using Hue. $Gray_3$ and $Gray_4$ may have abrupt intensity spatial variations that are not considered for this purpose.

From this intensity distribution it is possible to determine pressure values based in previous works. In this work, a proportional allocation was used, as proposed in [2], where the person's weight (w=m.g, product between mass and gravity acceleration) is distributed according to each pixel value by means of equation 8, proposed by Buchelly et al. [2].

$$P(x,y) = \frac{m.g}{A_{pixel}} \frac{I_{green}(x,y)}{\sum_{x=0}^{w}\sum_{y=0}^{h} I_{green}(x,y)} \quad (8)$$

Mayorca [5] shows that pressure versus intensity dependency present high correlation, so the dependency is linear. In our work, we use equation 8 because a linear dependency can be transformed to a proportional allocation performing an offset compensation.

4. Results and Discussion

In this work, the proposed system is evaluated with images of 11 different people footprints including children, adult men and adult women. The footprint image segmentation of a left foot is presented as an example in Figure 5, as well as its intensity distribution.

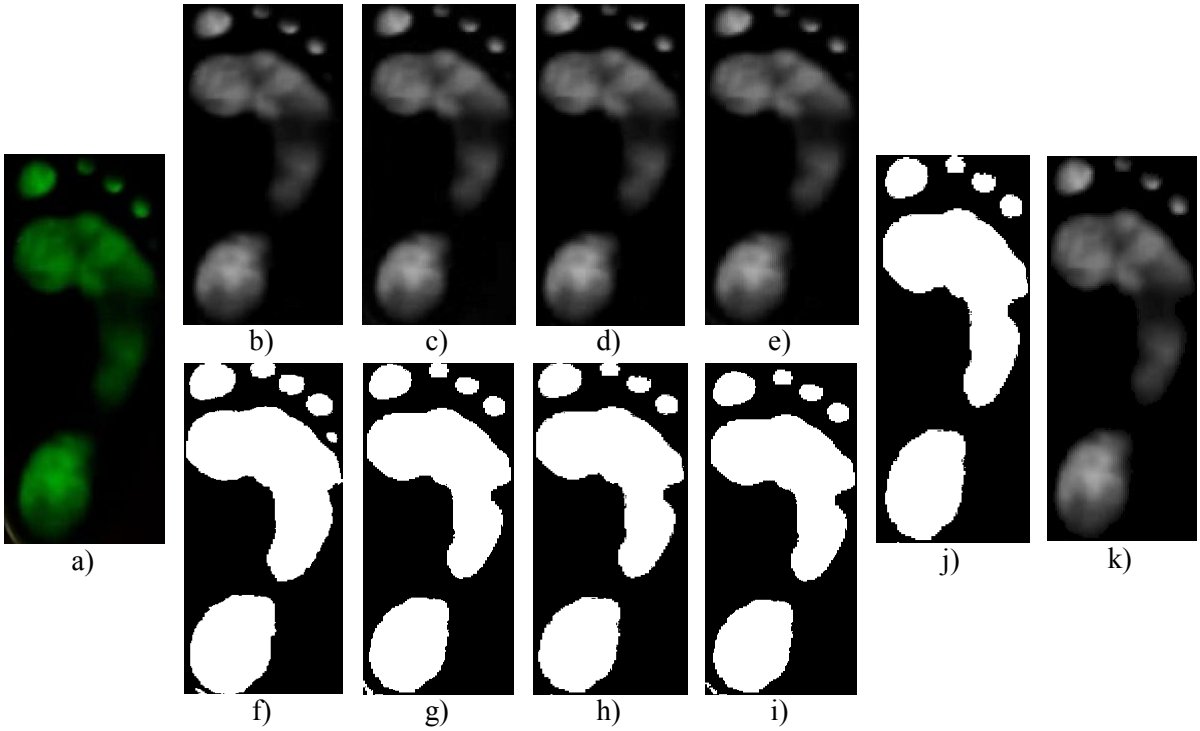

Figure 5. Footprint segmentation and intensity distribution: a) Part of the original image corresponding to a left foot, b) $Gray_1$, c) $Gray_2$, d) $Gray_3$, e) $Gray_4$, f) to i) binary images obtained by thresholding, j) AND operation between the binary images and k) intensity distribution.

The procedure applied for obtaining the final mask was simplified by thresholding only $Gray_1$ image, like the approach of [11]. However, some undesired green regions are captured (figure 5f) to 5i) near the heel) that may be large or small. In [11], those blobs were deleted after size and form analysis. In our work, they were eliminated or attenuated using the AND operation. If undesired regions remained, they were removed by means of morphological opening and closing.

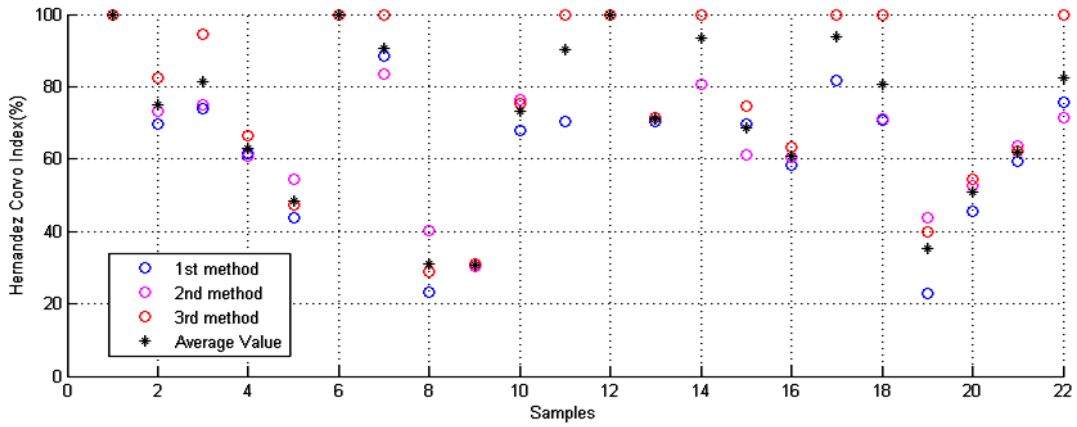

Figure 6. Comparison of the three methods for determining HC index and the average value. First half of data are right feet and second half are left feet.

In order to calculate the HC index, three mentioned methods were used as described before and then the average was calculated. They present some differences, as shown in Figure 6; however, the performance of each method is similar to the others, showing a high correlation.

In the same way, the Manual calculation of HC index is performed and the mean deviation from each method respect to the manual result is calculated, as shown in Table 2.

Table 2. Comparing performances of the three methods for HC index calculation.

	Method 1	Method 2	Method 3	Average
Square root of the mean square deviation of each method respect to the manual procedure.	9.78%	9.78%	14.98%	9.43%

On the other hand, the pressure distribution is found using equation 5. As an example, figure 7 shows pressure distributions for a plane foot, a normal foot and a cavus foot.

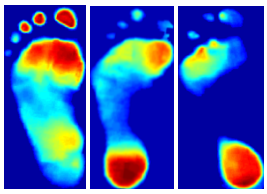

Figure 7. Pressure distribution of a plane foot (left) a normal foot (center) and a cavus foot (right).

The maximum and average values of pressure in each image varies depending on person's weight, foot size and foot type. Figure 8 shows the average pressure and the maximum pressure of each footprint.

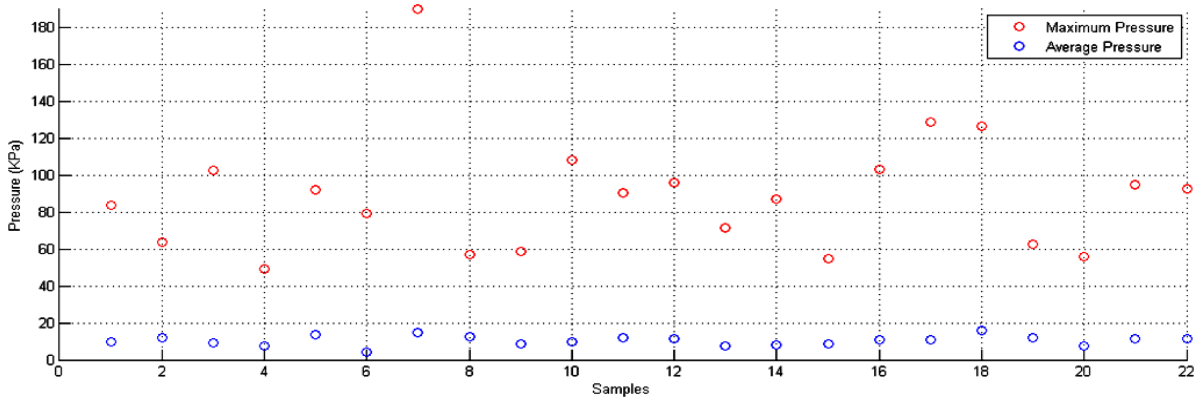

Figure 8. Mean and maximum pressure value for each sample foot.

Although the previous values are important for clinical assessments, a better diagnostic parameter may be the ratio between maximum pressure and mean pressure, because it measures the uniformity of the pressure distribution. In the analyzed samples, the minimum values of the ratio belong to the right and the left foot of the same person, and the HC index shows that both are plane. Additionally, this person is the younger child (samples 8 and 19 of figure 8). On the other hand, the maximum values of this ratio belong to extreme cavus feet (samples 6 and 17), showing high correlation with the HC index.

5. Conclusions

An automatic digital image processing system was created for detecting footprints from an optical pedobarograph for analyzing foot plant morphology and pressure distribution. Four transforms to gray scale were used for segmenting the footprint region with fixed thresholds. Definitive masks were obtained performing a logical AND operation that eliminates false detected binary objects. The

remaining undesired regions were removed and borders were smoothed by means of morphological opening and closing.

Length measures can be done using a conversion factor between physical lengths in centimeters and image lengths in pixels, as well as area measurements, for footprint morphological analysis in a binary mask. Hernandez Corvo assessment was performed automatically for twenty two samples (eleven persons) and classifying each foot as plane, normal or cavus in different grades. Three methods were used for determining HC index and the average value was calculated. These values were compared with the manual procedure and square mean deviation shows that the average value is the closest.

Combining the binary mask with the intensity image allows determining the pressure distribution on foot plant. Some descriptors like maximum pressure and mean pressure were calculated for each sample. The ratio between them measures the uniformity of the distribution and is independent of foot size and person's weight. Finally, pressure distribution and morphological classification of feet were compared to show the existence of high correlation between them.

The approach was methodologically appropriate for a preliminary work. As a future work we plan to build a protocol to evaluate it with a larger number of patients in order to validate clinically this technique.

6. References

[1] Revenga C and Bulo M 2005 El pie plano valgo: evolución de la huella plantar y factores relacionados *Revista Española de Cirugía Ortopédica y Traumatología* **49** 271-280

[2] Buchelly F, Mayorca D, Ramírez A, Mayorca H and Ferrín D 2009 *Elaboración de un podobarógrafo para análisis de la huella plantar* Fundación Universitaria María Cano (Popayán, Colombia: Proyecto de la asignatura de biomecánica para el programa de fisioterapia) p 1-32

[3] Oller A 2006 *La fórmula metatarsial y su valor predictivo en los trastornos de la marcha* Universitat de Barcelona (Barcelona: Tesis doctoral del programa de Doctorado Investigació en Ciències de la Salut) p 1-130

[4] Coll M, Viladot A and Suso A 1999 Estudio evolutivo del pie plano infantil *Revista española de cirugía ortopédica y traumatología* **43** 129-136

[5] Mayorca D 2011 *Diseño y construcción de un sistema óptico de análisis de distribución de presiones plantares para el diagnóstico de pie diabético mediante técnicas de visión por computador* Universidad del Cauca (Popayán, Colombia: Trabajo de grado de la carrera de Ingeniería Física) p 1-74

[6] Vélez M 2009 "Posturología como análisis preventivo de lesiones músculo-esqueléticas." *Empresa Preven-Ergo (Quito-Ecuador)* 1-5

[7] Aguilar I, Sánchez I, Pedraza G and Guadarrama L 2012 Correlación plantar y maloclusión. Caso clínico. *Revista ADM* **49** 91-94

[8] Pinzón M *Podología Unos pies sanos son la base de un cuerpo sano* BENAmedic clínica web page: http://www.clinicabenamedic.com/podologia/ Access date: 05-06-2015

[9] Lara S, Lara A, Zagalaz M and Martínez E 2011 Análisis de los diferentes métodos de evaluación de la huella plantar *Retos. Nuevas tendencias en Educación Física, Deporte y Recreación* **19** 49-53

[10] Berdejo D, Lara A, Martínez E, Chacón J and Lara D 2013 Footprint modifications according to the physical activity practised *Rev.int.med.cienc.act.fis.deporte* **vol. 13 num. 49** 19-38

[11] Ferrín D, Magdalena X and Loaiza H 2013 Determinación semiautomática de parámetros morfológicos de la huella plantar mediante el procesamiento digital de imágenes *Revista S&T* **11(27)** 9-26

[12] Arcan M and Brull M 1976 A fundamental characteristic of the human body and foot. The foot-ground pressure pattern *J. Biomechanics* **9** 453-457

[13] Lord M 1981 Foot pressure measurement: A review of methodology *Journal of Biomedical Engineering* **3** 91-99
[14] Bates K, Savage R, Pataky T, Morse S, Webster E, Falkingham P, Ren L, Qian Z, Collins D, Bennett M, McClymont J and Crompton R 2013 Does footprint correlate with foot motion and pressure? *Interface. Journal of the royal society* **10(83)**
[15] Arce C 2015 *Arces Software* Dr. Carlos Alberto Arce Gonzales, Medio especialista en medicina de rehabilitación http://www.arcesw.com/principal.htm Acces date: 05-07-2015
[16] Salazar C 2007 Pie plano, como origen de alteraciones biomédicas en cadena ascendente *Fisioterapia* **29(2)** 80-89
[17] Curvale G and Rochwerger A 2002 *Encyclopédie Medico-Chirurgicale E-14-429* Subject title: Pie cavo. Editions Scientifiques et Médicales Elsevier SAS (París)
[18] Zurita F, Martínez A and Zurita A 2006 Influencia de la tipología del pie en la actividad físico deportiva *Fisioterapia* **29(2)** 74-79
[19] López G and Coloma S 2012 Hallux valgius y presión plantar. Revisión de la literatura *I simposio sobre biomecánica y pie durante la actividad física – Universitat de Valencia (3-4 de Mayo de 2012)*
[20] Tizón E, Dovale M, Fernández C, López M, Mouteira M, Penabad S, Rodríguez O and Vásquez R 2004 Atención de enfermería en la prevención y cuidados del pie diabético *Aten Primaria* **34(5)** 263-271
[21] Tazi O and Debure C 2011 *Encyclopédie Medico-Chirurgicale E – 98-866-B-10* Subject title: Pie diabético. Editions Scientifiques et Médicales Elsevier SAS (Paris)
[22] Gómez E, Levy A, Díaz A, Cuesta M, Montañez C and Calle A 2012 Pie diabético *Seminarios de la fundación española de Reumatología* **13(4)** 119-129
[23] Díaz C, Torres A, Ramírez J, García L and Álvarez N 2006 Descripción de un sistema para la medición de las presiones plantares por medio del procesamiento de imágenes. Fase I *Revista EIA* **6** 43-55
[24] Shah S and Patil K 2005 Processing of foot pressure images and display of an advanced clinical parameter PR in Diabetic Neuropathy *Proceedings of the 2nd international IEEE EMBS conference on Neural Engineering Arlington, Virginia March 16-19, 2005* p v-viii
[25] Periyasamy R, Mishra A, Anand S and Ammini A 2010 Static foot pressure image analysis for variation in men and women while standing. Foot Pressure image analysis *Proceedings of 2010 international conference on systems in medicine and biology 16-18 December 2010, IIT Kharagpur, India* p 386-391
[26] Szeliski R 2010 *Computer Vision: Algorithms and Applications* Springer p 327-342
[27] Ferrín C and Buchelly F 2010 *Diseño y construcción de plataformas multitoque de tipo óptico, utilizando técnicas de visión artificial en tiempo real, para facilitar la interacción de los usuarios con el computador* Universidad del Cauca (Popayán, Colombia: Trabajo de grado de la carrera de Ingeniería Física) p 28-31
[28] 2009 *Opencv 2.0 Documentation* p 313
[29] Gonzalez R and Woods R *Digital image processing (Second Edition)* Prentice Hall (Upper Saddle River, New Jersey) p 528-531

Acknowledgments
Authors acknowledge the assistance from the GOL members (Grupo de Optica y Láser) of Universidad Del Cauca, especially to engineers Leonairo Pencue Fierro and Carlos Diego Ferrín.